Proton-Transfer Mechanism for Dispersed Decay Kinetics of Single Molecules Isolated in Potassium Hydrogen Phthalate

Eric D. Bott, Erin A. Riley, Bart Kahr,* and Philip J. Reid*

Department of Chemistry, University of Washington, Box 351700, Seattle, Washington 98195

ABSTRACT The excited-state decay kinetics of single 2′,7′-dichlorofluorescein (DCF) molecules oriented and overgrown within crystals of potassium acid phthalate (KAP) are reported. Time-correlated single-photon counting measurements (TCSPC) of 56 DCF molecules in KAP reveal that single-exponential decay is exhibited by roughly half of the molecules. The remainder demonstrates complex excited-state decay kinetics that are well fit by a stretched exponential function consistent with dispersed kinetics. Histograms of single-molecule luminescence energies revealed environmental fluctuations and distinct chemical species. The TCSPC results are compared to Monte Carlo simulations employing a first-passage model for excited-state decay. Agreement between experiment and theory, on both bulk and single-molecule levels, suggests that a subset of the DCF molecules in KAP experience fluctuations in the surrounding environment that modify the energy barrier to proton transfer leading to dispersed kinetics.

KEYWORDS: single molecule microscopy · dispersed kinetics · fluorescence lifetime · fluorescence intermittency · proton transfer

Single-molecule (SM) spectroscopies have made plain previously hidden phenomena such as quantum jumps,[1] photon antibunching,[2] spectral diffusion,[3] and of special interest herein fluorescence intermittency,[4−15] or "blinking". Blinking refers to the observation that emission from a SM under continuous excitation switches between emissive (*i.e.*, *on*) and nonemissive (*i.e.*, *off*) periods. The temporal duration of these events varies from submilliseconds to minutes.[4] The identification of the nonemissive state that is produced and the factors that define the population and depopulation kinetics of this state remain equivocal for many systems. Nevertheless, fluorescence intermittency provides a way to directly interrogate chromophore electronic properties in complex environments. Moreover, the nonemissive states that are populated may serve as gateway states for material photodecomposition.[16−18] Identifying the nature of these states and developing strategies for limiting their production provides a rational pathway toward the development of more robust chromophoric materials. If the pathways for blinking can be understood and controlled, then significant advancements in the use of single emitters as probes of chemical and biochemical phenomena may be achieved.

The underlying photophysics responsible for fluorescence intermittency can be approached by computing autocorrelation functions or by compiling and analyzing histograms of *on*- and *off*-time durations.[11] For some systems, the *on*- and *off*-time distributions are described by simple, single-exponential functions that are directly related to the rate constants for population and depopulation of a nonemissive triplet state.[1,19,20] Pentacene molecules in *p*-terphenyl crystals demonstrate *on*- and *off*-time distributions that are exponential, consistent with triplet state population and decay.[21] Similarly, the *off*-time histograms for $DiIC_{18}$ molecules in poly(methyl methacrylate) and polystyrene were fit by single exponentials that are consistent with the triplet lifetime.[22] However, many other systems demonstrate *on*- and *off*-time distributions that are not single-exponential. In particular, the blinking statistics of single semiconductor nanocrystals or quantum dots (QDs) are generally complex,[4,15] as well as many luminescent dyes.[5,23−26] For these systems, the *on*- and *off*-time histograms follow the form $P_{on/off} \propto t^{-m}$ where m is the power-law exponent.[4] The observation of power laws is consistent with distributed kinetics in which the population/depopulation rate constants are not well described by a single value, but instead vary with time, and have been successfully modeled with Monte Carlo (MC) simulations.[23,27,28]

*Address correspondence to preid@chem.washington.edu, kahr@chem.washington.edu.

Received for review June 5, 2009 and accepted July 28, 2009.

Published online August 6, 2009.
10.1021/nn900596a CCC: $40.75

Etiologies proposed for distributed kinetics in organic chromophores have included molecular rotation, conformational flexibility, spectral diffusion, reversible photo-oxidation, and intermolecular electron transfer.[4] Recent advances have been made toward the control of blinking and the identification of chemical and photochemical processes that result in reversible reactions which render a molecule nonemissive. These mechanistic investigations are advancing a promising technique, photoswitching microscopy, in which light is used to selectively turn molecules *on* and *off* and ultimately enables one to image objects with subdiffraction limit resolution.[29] For many of these photoswitchable molecules the mechanisms for switching have been identified. For some molecules, multiple mechanisms have been proposed. One particularly interesting example is the photoswitching of Dronpa, a protein closely related to green-fluorescent protein, *via* a cis−trans isomerization in conjunction with protonation/deprotonation of the chromophore.[30] Success has also been achieved with synthetic chromophores by tailoring molecular environments to change the reduction and oxidation potential for ionization reactions.[31−33] Researchers are actively trying to establish the nature of the QD dark state, as well,[15] with similar blinking modifications being achieved through refined engineering of core/shell boundaries.[34] Although there is general agreement that blinking is an intrinsic characteristic of SM emission, ambiguity persists regarding the mechanisms of dark-state population and depopulation.

We have taken the unique approach of studying the blinking dynamics of organic luminophores isolated in single crystals of potassium acid phthalate (KAP).[23,35−39] Crystals provide well-defined environments in which to investigate SM photophysics since the lattice is ordered and restricts molecular translation and rotation. An added advantage of the crystalline matrix is the reduction of irreversible chromophore photodecomposition due to processes such as photo-oxidation is reduced. The enhancement in photostability provided by the crystal prolongs the time over which emitters may be studied.[35,40,41] Previously, we observed power-law blinking on single dye molecules in KAP for both *on*- and *off*-times with exponents of $m_{on/off} \approx 1.5$. Spectral diffusion of SM in KAP has also been observed, and correlations between spectral jumps and intensity fluctuations are widely reported for both organic chromophores and QDs.[4,38,42,43] Theoretically, spectral diffusion and blinking phenomena have been connected for quantum dots using first-passage theory and successfully reproduced a power-law exponent of 1.5.[44] In this approach, electron transfer was promoted as the most likely mechanism; however, first-passage theory can be used to describe other chemical processes. Moreover, different analyses of identical data have been shown to significantly alter the power-law fit parameters.[38] While first-passage theories are attractive, the weak association of mechanisms to blinking statistics for complex systems underscores the need for auxiliary analytical methods for deeper analysis of SM photophysics.

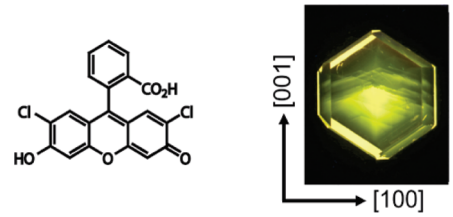

Figure 1. Example dye-inclusion KAP crystal. 2′,7′-Dichlorofluorescein incorporates into the fast slopes of growth hillocks within the {010} growth sector of KAP, as evidenced by emission photographs of heavily-doped crystals.

Blinking provides a measure of dynamics that occur on relatively long time scales (≥1 ms), but it is unclear if dispersed kinetics extend to shorter times. The limited amount of information available suggests dispersive kinetics are manifested on shorter time scales, as well. For example, MC simulations predict that decay of the optically prepared excited state should demonstrate kinetic dispersion.[23] Extrapolation of autocorrelated QD data also suggests that blinking dynamics are manifest at nanosecond time scales,[45] in correspondence with macroscale blinking traces. A few studies have directly measured the excited-state lifetime of individual quantum dots and have found dispersion evidenced by nonexponential excited-state decay.[12,46−48] Does a similar scaling of distributed kinetics exist for mixed crystals? To address this question, we report here the measurement of single-molecule fluorescence lifetimes of 2′,7′-dichlorofluorescein (DCF) in KAP (Figure 1) employing time-correlated single-photon counting (TCSPC). We find that, for a significant subset of the DCF molecules, the decay kinetics for the lowest-energy excited singlet state are dispersed, as evidenced by nonexponential decay of the optically prepared excited state. In addition, the spectral diffusion of DCF in KAP is studied, and energy-shift histograms were constructed and analyzed. The excited-state decay kinetics were reproduced by MC simulations using first passage theory, where the energy barrier between the optically prepared excited state and a dark state is modified stochastically using the experimentally obtained energy shift probability distribution. Careful analysis of the optical and photochemical properties of DCF in KAP supports a photoinduced proton-transfer mechanism for distributed kinetics and dark-state population and depopulation.

RESULTS AND DISCUSSION

SM lifetimes were determined from TCSPC decay histograms, analogous to bulk fluorescence lifetime measurements by the ergodic hypothesis. SM lifetimes represent a convolution of both radiative and nonradiative transitions from the optically prepared excited state ($|2\rangle$), to the singlet ground state ($|1\rangle$), and

nonemissive state (|3⟩). Molecular fluorescence governed by time-invariant first-order kinetics predicts decay histograms best fit to single-exponential functions with a lifetime of $\tau = (k_{23} + k_{21})^{-1}$. Distributed values of k_{23} result in varying fluorescence lifetimes. Thus, the fluorescence decay curve will be best represented by a stretched exponential function of the form

$$F \propto e^{-(t/\tau_{KWW})^{\beta}} \quad (1)$$

where τ_{KWW} is the Kohlrausch, Williams, and Watts characteristic relaxation time[49] and β is the stretching parameter bound by 0 and 1. A β value of 1 corresponds to single-exponential decay, with a decrease in β reflecting increased nonexponential decay kinetics. The fit values of τ_{KWW} and β were reduced to a single decay parameter τ_c as follows:

$$\tau_c = \frac{\tau_{KWW}}{\beta}\Gamma\left(\frac{1}{\beta}\right) \quad (2)$$

where $\Gamma(x)$ is the gamma function.

Fluorescence decay histograms obtained for 56 SMs of KAP/DCF were analyzed in order to assay the prevalence of distributed fluorescence kinetics. Figure 2 depicts three normalized SM TCSPC histograms with corresponding best fits. Displayed on a semilog axis, it is apparent that Figure 2a is best represented by a single-exponential function (β = 1), whereas the decay

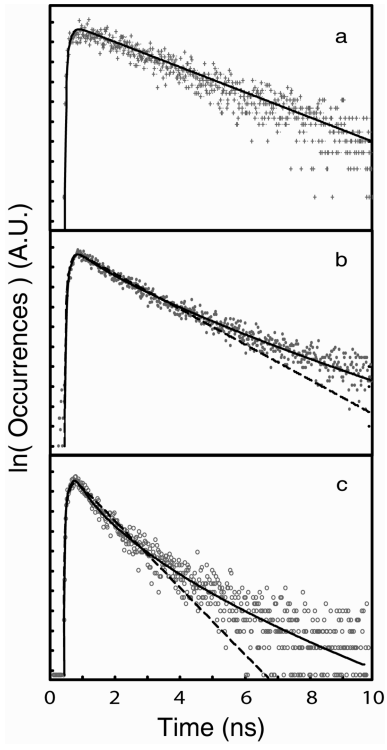

Figure 2. Three KAP/DCF single-molecule lifetime histograms on semilog plots with stretched exponential fits (solid) overlaid, along with single-exponential fits (dashed) on (b) and (c) for contrast. Decreasing β fit parameters manifest as deviation from linear decay. Values of β are (a) 1, (b) 0.75, and (c) 0.57.

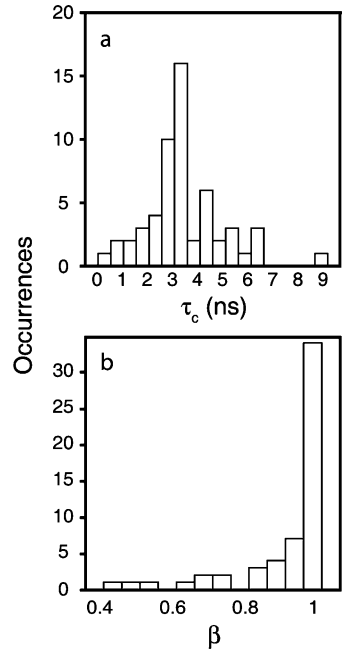

Figure 3. (a) Histogram of τ_c fit parameters for 56 single molecules of KAP/DCF. The distribution spans 0.58−9.2 ns, with an average of 3.6 ± 1.5 ns. (b) Histogram of β fit parameters for 56 single molecules of KAP/DCF; 55% of the molecules deconvolved to a β value of 1, denoting single-exponential decay. The remaining 45% deconvolved to a range of β values, down to 0.46.

profiles in Figure 2b,c deviate from a straight-line fit and are instead better represented by a stretched exponential (β ≠ 1). Histograms of β and τ_c for 56 individual molecules of KAP/DCF are shown Figure 3. Best-fit values of β span 1 to 0.46. Values of τ_c range from 0.6 to 9.2 ns with an average value of 3.6 ± 1.5 ns. For comparison, DCF exhibits an excited-state decay lifetime of 2.46 ± 0.05 ns in ethanol and 3.61 ± 0.05 ns in a heavily dyed KAP crystal.

The TCSPC distribution of β values reveals stretched exponential decays of the optically prepared excited state for nearly half of the DCF molecules (see Figure 3b). For these molecules, excited-state decay is not represented by a single time constant, but a convolution of many. Previously, luminophores in KAP yielded power-law histograms of *on*- and *off*-times, indicative of distributed kinetics at the millisecond/minute time scales.[23] Therefore, excited-state distributed kinetic processes are manifest over nine decades in time. To the authors' knowledge, this is the first report of rate dispersion over such long time scales for organic molecules. However, similar results have been reported for single QDs, where Sher *et al.* found that a common power-law coefficient described the excited-state decay as well as the blinking dynamics.[46] Additionally, dispersed excited-state decay kinetics have been observed for tethered core/shell QDs in a microfluidic channel,[50] QDs located near silver nanoislands on a quartz surface,[51] and QDs imbedded in PMMA films.[48] Fascinatingly, CdSe/ZnS QDs have also shown nonexponential life-

times within individual intensity segments of fluorescence traces.[12,52] Current interest in this area of research is to identify the physical processes responsible for dispersed kinetic behavior on the nanosecond and longer time scale and to ascertain if a single process is responsible for this behavior over such a wide variety of time scales.

Distributed rate constants for fluorescence intensity switching between *on* and *off* are often associated with environmental heterogeneity. Power-law histograms are frequently recreated in intermolecular charge-transfer models by employing static, random distributions of trapping sites in the surrounding matrix.[28] For this reason, it was not believed that distributed kinetics (at any time scale) would be observed in homogeneous host matrices.[4] It is therefore surprising that a variety of luminophores in KAP exhibit this phenomenon. Room temperature spectral diffusion measurements of chromophores in KAP may provide insight into why homogeneous host matrices exhibit dispersed kinetics on both fluorescence and blinking time scales. Correlations between spectral jumps and intensity jumps have been made for both QDs[42] and organic chromophores.[43] It is accepted that environmental fluctuations alter excited-state energetics, resulting in observed SM spectral diffusion.[53] Such fluctuations also promote energy-barrier crossing along adiabatic reaction coordinates. Evidence for this pathway was found in temperature-dependent blinking studies of organic dyes in polymer hosts.[54]

The energy distribution for SMs of DCF in KAP was measured as for violamine-R (VR).[38] The emitted photons from SMs of DCF in KAP were separated by color with a dichroic mirror centered at the bulk emission maximum. The combined intensity for each blinking trace was deconvolved using a change-point detection algorithm,[55] and the spectral energy shifts were calculated for every deconvolved segment based upon the average intensity ratio between the detectors. Histograms of energy-shift occurrences are shown in Figure 4a. The energy distribution in Figure 4b corresponds to the distribution in Figure 4a weighed by segment duration to create a temporal-probability distribution of energy shifts. Figure 4c was calculated by using the total number of photons emitted from each occurrence shown in Figure 4a. This distribution best corresponds to the ensemble fluorescence. We used the time-weighted energy-shift probability distribution (Figure 4b) as a measure for the energy fluctuations in the dielectric to reproduce the TCSPC results discussed above.

To relate the fluorescence decay measured by TCSPC to an underlying physical process, we performed Monte Carlo (MC) simulations similar to the approach employed to investigate the blinking dynamics of VR in KAP.[23] The model consists of a three-level system with distributed kinetics describing population and depopulation of a third (*e.g.*, dark) state. One of the central findings in our studies of luminophores isolated in KAP was that the environment around the SMs fluctuates with time, as evidenced by spectral diffusion of VR[38] and DCF in KAP. If these fluctuations promote population and depopulation of the dark state, then one would expect that the experimentally observed distribution of SM emission energies to be related to the distribution of dark-state population and depopulation rates. Marcus and Tang have investigated the role of spectral diffusion in QD blinking and developed the diffusion-controlled electron transfer (DCET) model for quantum dot blinking.[44] Here, individual emitters (or molecules) experience time-dependent fluctuations in the surrounding dielectric that alter the energy barrier separating the optically prepared excited state from the dark state (Figure 5). This time-dependent modification of the barrier height gives rise to distributed kinetics and

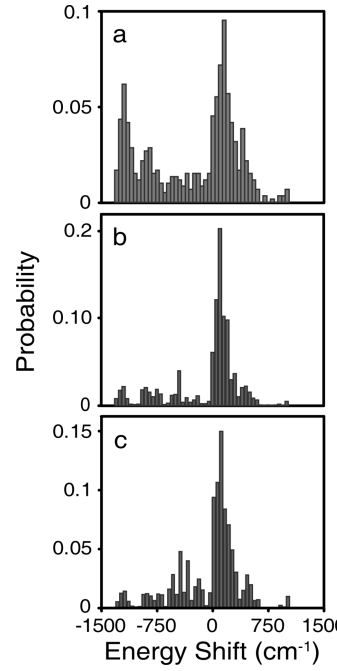

Figure 4. Energy probability histograms obtained for the single-molecule obtained by filtering the emission with a dichroic mirror, with (a) each deconvolved segment equally weighted, (b) weighted by segment duration, (c) weighted by total photons emitted.

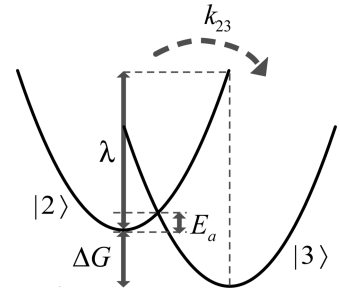

Figure 5. Marcus scheme for the first-passage model: λ is the energy required for the reactant state to arrive at the product geometry without reaction; ΔG is the free energy difference between product and reactant states; and E_a is the energy barrier separating the reactants and products.

a corresponding power-law distribution of *on*- and *off*-times.[23] The underlying principles of the DCET model can easily be extended to other barrier-mediated processes such as proton transfer mechanisms (see below). The power-law description of *on* and *off* events for luminophores in KAP makes a first-passage model attractive.

The first-passage model is based on Marcus theory, where the rate for barrier crossing depends on the reorganization energy (λ) and the free energy difference (ΔG) between the reactant and product states (Figure 5). These quantities combine to establish the activation energy, E_a, and corresponding rate constant expressed in its familiar Arrhenius form:

$$E_a = \frac{(\lambda + \Delta G)^2}{4\lambda} \quad (3)$$

$$k = Ae^{-E_a/k_BT} \quad (4)$$

Equations 3 and 4 provide a direct connection between fluctuations in ΔG and dispersed kinetics, with the extent of rate constant dispersion depending not only on the distribution of ΔG but also on the value of ΔG relative to the reorganization energy. The time-weighted energy shift histogram (Figure 4b) represents the probability that a certain energy shift is sampled at a given moment; therefore, this distribution was employed in the MC simulations with energy shifts (δ) serving as the MC variable. In the simulation, the molecule is prepared in the optically excited state $|2\rangle$, with predetermined values for the fluorescence rate constant k_{21}, ΔG, λ, the prefactor A, and the free energy gap shifted by an amount δ. The rate constant for reactant state decay, k_{23}, is then calculated with reference to δ:

$$k_{23} = Ae^{-(\lambda + \Delta G + \delta)^2/4\lambda k_BT} \quad (5)$$

Once the rates are determined, the transition probability from $|2\rangle$ is calculated at progressive time steps, t = 20 ps, and compared to a random number chosen from a uniform distribution.

$$P_{|2>} = 1 - e^{-(k_{21}+k_{23})t} \quad (6)$$

At the time a transition is made, the reaction pathway is chosen by comparing the fluorescence quantum yield to a random number:

$$\phi_f = \frac{P_{|1>}}{P_{|3>} + P_{|1>}} = \frac{k_{21}}{k_{21} + k_{23}} \quad (7)$$

If the fluorescence pathway is chosen, the arrival time is recorded; otherwise, the process starts over with a new δ value. Five values of ΔG (λ/4, 0, −λ/4, −λ/2, −λ) were investigated. Most of these values correspond to the "normal" Marcus regime except for $\Delta G = -\lambda$, which represents a barrierless process. In the absence of specific information regarding the reorganization energy, a typical value of 0.2 eV was employed. The simulations were also carried out with λ = 0.4 eV with no impact to the conclusions presented here. Finally, k_BT = 200 cm^{-1} and $k_{21} = 3 \times 10^{-8}$ s^{-1}, consistent with earlier work.[23] The simulation was run for a variety of pre-exponential values, A, for 10^4 total photon emission events. Decay histograms were fit using a nonlinear least-squares fitting routine to the stretched exponential function (eq 1).

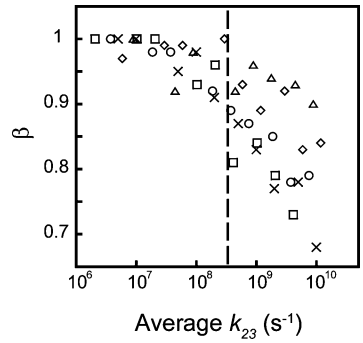

Figure 6. Dependence of stretching parameter, β, on average rate, or pre-exponential factor, of k_{23} for $\Delta G = \lambda/4$ (cross), $\Delta G = 0$ (square), $\Delta G = -\lambda/4$ (circle), $\Delta G = -\lambda/2$ (diamond), and $\Delta G = -\lambda$ (triangle). Stretching occurs at k_{23} rates of comparable magnitude or greater than k_{21}.

For all five chosen values of ΔG, there was little to no variation of the best fit value of τ_{KWW} from stretched exponential fitting of the MC−TCSPC curves, though the magnitude of the stretching parameter, β, changed significantly. Figure 6 presents the best fit β values *versus* the average rate for each value of ΔG. For barrierless crossing ($\Delta G = -\lambda$), effectively no stretching is observed, and as ΔG diminishes to enter the normal regime, the magnitude of β decreases significantly from unity. The simulated decay curves at $\Delta G = \lambda/4$ are best represented by β values approaching 0.7, consistent with experiment.

The MC simulations demonstrate that the average dark-state transition rate must be comparable to the fluorescence decay rate, and that the reaction barrier must be comparable to the environmental energy fluctuations to recreate the observed dispersion. In contrast, dark-state population rate constants employed in basic trapping style blinking models are several orders of magnitude slower than the rate constant for fluorescence[4,28] and, therefore, cannot alter the effective fluorescence lifetime of the molecules. The simulations were able to reproduce the wide range of TCSPC results, suggesting that inherent differences in site per site energetics could be the cause for both the large population of dyes that do not exhibit distributed kinetics and those that do.

Given the TCSPC results coupled with the MC simulations, we can conclude that the dispersed fluorescence kinetics for single molecules can be reproduced with a first-passage theory. What remains unclear is the photophysical processes responsible for the dispersed

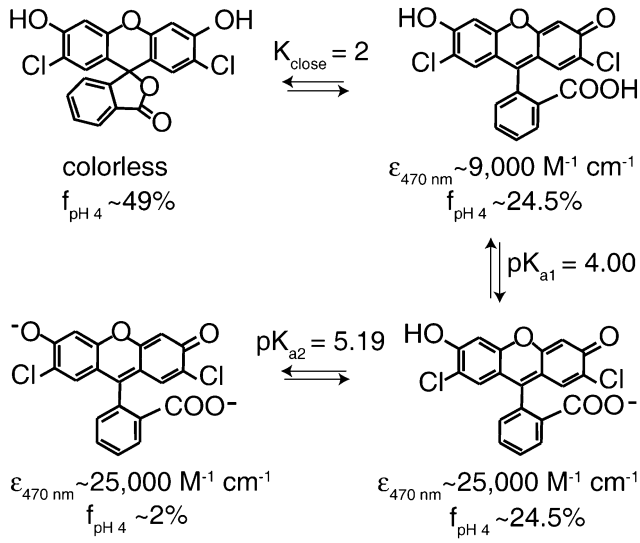

Figure 7. Different protonation forms of DCF with partition coefficients and estimated molar absorptivities at 470 nm at pH = 4. Clockwise, from top left, is the lactone, quinoid, anionic, and dianionic forms. In addition, ε is the molar extinction coefficient and f is the fractional concentration at pH 4.

kinetics observed here. In order to address this question, a detailed understanding of the photochemical and fluorescence properties of DCF is required. In KAP solution, DCF exists as an equilibrium of four dominant species: quinonoid, neutral lactone, monoanionic, and dianionic forms shown in Figure 7. The respective equilibrium constants, approximate molar absorptivities at 470 nm, and the fraction of molecules expected in a saturated KAP solution (pH = 4) are also shown.[56] Each species has its own characteristic absorption and fluorescence spectrum, all of which overlap, as demonstrated in the pH-dependent absorbance and emission of DCF in water and in saturated (0.5M) KAP (Figure 8). In basic and neutral solutions, the dianion is the dominant species. As the pH decreases, the monoanion appears as evidenced by an isosbestic point at ~460 nm.

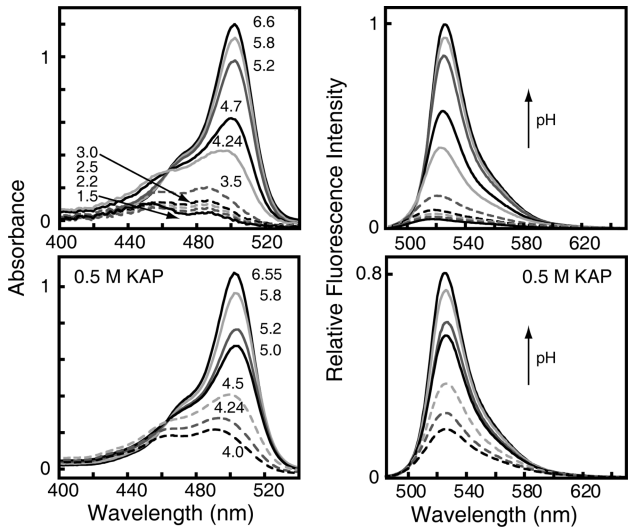

Figure 8. Absorption and emission properties of DCF in water and saturated KAP solutions *versus* pH.

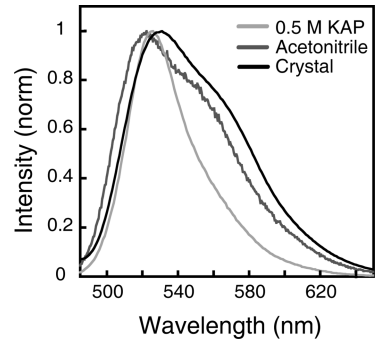

Figure 9. Bulk fluorescence of DCF in KAP, along with DCF in acetonitrile and saturated KAP solution. The crystal emission profile most closely resembles the polar aprotic environment given by acetonitrile.

As the pH is lowered, the population of the dianion decreases, and the neutral and monoanion forms remain. No further isosbestic point is observed as depletion of the neutral compound occurs to form the lactone structure, and this species is colorless.[57] As pH is decreased and the neutral species are favored, fluorescence intensity is reduced, consistent with the evolution of the molar absorptivities between the various forms shown in Figure 7. In KAP solutions, the dye equilibrium shifts to the neutral configurations, as evidenced by absorbance change in Figure 8. The fluorescence of the dye in KAP solutions is quenched by ~10% as compared to aqueous solutions (Figures 8), indicating that KAP provides a weak perturbation of the dye's electronic structure.

The fluorescence spectra for all forms of the dye in aqueous solutions are similar, but marked broadening and a large shoulder on the red edge of the band become apparent when the neutral compound is favored. There are significant differences between the DCF spectra from the saturated KAP solution and the KAP crystal. The fluorescence of a heavily dyed KAP crystal is shown in Figure 9, and for comparison the dye in acetonitrile and in 0.5 M KAP. In acetonitrile, the dye is in the lactone and quinonoid forms; the luminescence spectra resemble that in the KAP lattice. Previous studies of DCF in KAP have shown the existence of both deprotonated and neutral species within heavily dyed crystals.[37] Furthermore, we have SM evidence of both the quinonoid and deprotonated species within KAP. The fluorescence intensity maximum for DCF shifts by roughly 1300 cm^{-1} between polar-aprotic and aqueous solutions (where the anionic form is dominant), and the same separation is evident in the segment-weighted energy-shift histogram (Figure 4a), consistent with both forms in KAP at the SM level. Photoinduced proton-transfer mechanisms may promote interchange between populations with different molar extinction coefficients, the etiology for intensity fluctuations, and long-lived dark states. To extrapolate our mechanistic understanding of fluorescence dispersion to the processes operative in blinking, we are performing correlated measurements of fluorescence lifetimes

and blinking for DCF in KAP, and the results of this work will be reported shortly.

Electron transfer is the dominant hypothesis for complex blinking of organic chromophores.[4,58] However, several features of DCF in KAP suggest that electron transfer may not be the underling mechanism of blinking. Flash photolysis of fluorescein dyes in solution showed oxidized and reduced ions, but neither of these is stable and quickly reform the parent species.[59] For electron transfer to be responsible for a long-lived dark state, the radical species must be stabilized as in R6G-PVA dye host,[58] but this condition is not supported for DCF. Finally, DCF may be photo-oxidized and reduced in the presence of strong oxidizing and reducing agents,[60,61] though neither of which is present in the oxygen impermeable KAP environment. While DCF does not fit into the electron-transfer scheme, it does have a wealth of proton chemistry that may explain distributed kinetics of DCF in KAP using the same first-passage formalism as invoked in DCET.

Photoinduced proton transfer of a related dye, 2′,7′-difluorofluorescien, has been reported in acetate solutions,[62−64] a buffer like KAP. However, to assess the possibility of proton transfer within KAP crystals, the solid-state properties must be considered. The crystal structure of KAP consists of bilayers. These sheets are bound by weak van der Waals interactions which are responsible for the mica-like structure of the crystal. Within each sheet, the monomers are tightly bound in a herringbone arrangement through carboxylate−carboxylic acid hydrogen bonds. The AC conductivity of KAP is consistent with an activation energy of 0.022 eV at 1 kHz,[65] a low barrier for charge-carrier hopping. Since the crystal consists of hydrogen bonds, the electrical transport in KAP is believed to involve proton tunneling across the layered sheets. Previous studies of DCF in KAP have shown that the main driving force for incorporation is carboxylate for carboxylate (or carboxylic acid for carboxylic acid) substitution wherein the dye is directly substituted into the hydrogen-bond network of the crystal.[37] The dye's direct access to this low-energy proton-transfer channel within the crystal strongly supports the notion of solid-state proton transfer between the dye and crystal. A popular study on complex blinking of R6G in PVA ruled out proton transfer because strong coupling leads to fast rate constants.[58] However, the TCSPC−MC results illustrate that to reproduce distributed kinetics at short times this is precisely what is needed. The lattice properties of KAP may explain the creation of long-lived dark states since proton tunneling rates are much slower. Proton-transfer chemistry can account for both fast and slow excited-state kinetics for DCF in KAP.

CONCLUSION

Single-molecule lifetimes of DCF in KAP were measured by TCSPC and revealed large diversity where half of the molecules exhibited stretched exponential decay of the optical excited state. This surprising result shows that host heterogeneity is not solely responsible for dispersed excited-state kinetics at any time scale for organic molecules. Measurements of the SM energy profile of DCF molecules in KAP and the observation of spectral diffusion are evidence for fluctuations in the dielectric that may serve to promote dark-state population and depopulation. First-passage theory was used to model TCSPC results, where the reaction barrier height needed to be of similar magnitude as the spectral energy shift distribution. These simulations recreated the range of experimentally observed excited-state decays. Though the mechanism of electron transfer was discussed, the photochemical properties of both DCF and KAP overwhelmingly support a proton-transfer mechanism for dark-state population and depopulation.

METHODS

Dye-inclusion crystals were grown by evaporation of supersaturated, aqueous KAP (Aldrich) solutions containing 10^{-8} M DCF (Aldrich) maintained at 30 °C in a water bath. Crystals were cleaved parallel to the (010) face, attached to glass coverslips (Corning) with vacuum grease, and mounted in an inverted orientation on a closed loop $x-y$ piezo scanning stage (Queensgate, NPS-XY-100B). SM lifetimes were collected with an inverted confocal microscope (Nikon, TE2000U) and TCSPC electronics consisting of a nanosecond delay module and a time-to-amplitude converter (TAC, Canberra, 2145).[66] Individual KAP/DCF molecules were photoexcited using a 470 nm pulsed laser (Picoquant, PDL 800-B) having a temporal width of 63 ps (full width at half-maximum), a repetition rate of 1 MHz, and an average power of 67 nW. The excitation pulses were focused onto the sample through a 100× oil-immersion objective (Nikon, PlanFluor, 1.4 NA). Fluorescence photons were back-collected through the objective, filtered (Chroma, 480 LP) from the excitation field, and focused onto an avalanche photodiode detector (APD) with a 50 μm active area (MPD, PDM050CTB) providing confocal resolution. Synchronization pulses from the laser driver and photon event signals from the APD were sent to the TAC, with the TAC output binned using a multichannel analyzer (FAST ComTec, MCDLAP). Single-molecule luminescence decay histograms were derived using binning time delays between individual excitation, and emission events with ~10^4 excitation/emission time-delay pairs were acquired for each SM to construct a fluorescence decay histogram. The fits were optimized based on minimization of χ^2. Errors were determined from diagonal elements of the covariance matrix reported as 90% confidence assuming normally distributed errors.

Single-molecule energy-shift experiments were conducted as previously described,[38] except a dichroic mirror centered at 532 nm (Omega 540DRLP) was employed. Absorbance spectra were acquired on a SI Photonics CCD array UV−vis spectrometer. Fluorescence spectra were acquired on a Fluoromax-2 spectrophotometer. Sample pH values were determined using Venier LabQuest equipped with a pH sensor. For pH-dependent fluorescence measurements, a dye concentration of 6.78×10^{-6} M was employed. Accurate determinations of the molar absorptivities and fluorescence quantum yields for the neutral and monoanion forms of the dye are unavailable due to spectral

overlap. Fluorescence quantum yields have been reported for the dianion in 0.01 M aqueous NaOH (0.88)[57] and in an ethanol/benzene/water mixture (0.42).[57,67]

Acknowledgment. P.J.R. acknowledges support from the Center on Materials and Devices for Information Technology Research, a Science and Technology Center sponsored by the NSF (DMR- 0120967). B.K. also acknowledges support from the NSF (CHE-0349882).

REFERENCES AND NOTES

1. Basché, Th.; Kummer, S.; Bräuchle, C. Direct Spectroscopic Observation of Quantum Jumps of a Single-Molecule. *Nature* **1995**, *373*, 132–134.
2. Basché, Th.; Moerner, W. E.; Orrit, M.; Talon, H. Photon Antibunching in the Fluorescence of a Single Dye Molecule Trapped in a Solid. *Phys. Rev. Lett.* **1992**, *69*, 1516–1519.
3. Lu, H. P.; Xie, X. S. Single-Molecule Spectral Fluctuations at Room Temperature. *Nature* **1997**, *385*, 143–146.
4. Cichos, F.; von Borczyskowski, C.; Orrit, M. Power-Law Intermittency of Single Emitters. *Curr. Opin. Colloid Interface Sci.* **2007**, *12*, 272–284.
5. Hoogenboom, J. P.; van Dijk, E. M. H. P.; Hernando, J.; van Hulst, N. F.; García-Parajó, M. F. Power-Law-Distributed Dark States are the Main Pathway for Photobleaching of Single Organic Molecules. *Phys. Rev. Lett.* **2005**, 95.
6. Pirotta, M.; Güttler, F.; Gygax, H.; Renn, A.; Sepiol, J.; Wild, Urs. P. Single-Molecule Spectroscopy: Fluorescence-Lifetime Measurements of Pentacene in *p*-Terphenyl. *Chem. Phys. Lett.* **1993**, *208*, 379–384.
7. Dickson, R. M.; Cubitt, A. B.; Tsien, R. Y.; Moerner, W. E. On/Off Blinking and Switching Behaviour of Single Molecules of Green Fluorescent Protein. *Nature* **1997**, *388*, 355–358.
8. VandenBout, D. A.; Yip, W. T.; Hu, D.; Fu, D. K.; Swager, T. M.; Barbara, P. F. Discrete Intensity Jumps and Intramolecular Electronic Energy Transfer in the Spectroscopy of Single Conjugated Polymer Molecules. *Science* **1997**, *277*, 1074–1077.
9. Nirmal, M.; Dabbousi, B. O.; Bawendi, M. G.; Macklin, J. J.; Trautman, J. K.; Harris, T. D.; Brus, L. E. Fluorescence Intermittency in Single Cadmium Selenide Nanocrystals. *Nature* **1996**, *383*, 802–804.
10. Kuno, M.; Fromm, D. P.; Hamann, H. F.; Gallagher, A.; Nesbitt, D. J. Nonexponential "Blinking" Kinetics of Single Cdse Quantum Dots: A Universal Power Law Behavior. *J. Chem. Phys.* **2000**, *112*, 3117–3120.
11. Kuno, M.; Fromm, D. P.; Hamann, H. F.; Gallagher, A.; Nesbitt, D. J. "On"/"Off" Fluorescence Intermittency of Single Semiconductor Quantum Dots. *J. Chem. Phys.* **2001**, *115*, 1028–1040.
12. Zhang, K.; Chang, H.; Fu, A.; Alivisatos, A. P.; Yang, H. Continuous Distribution of Emission States from Single CdSe/ZnS Quantum Dots. *Nano Lett.* **2006**, *6*, 843–847.
13. Wang, S.; Querner, C.; Emmons, T.; Drndic, M.; Crouch, C. H. Fluorescence Blinking Statistics from CdSe Core and Core/Shell Nanorods. *J. Phys. Chem. B* **2006**, *110*, 23221–23227.
14. Glennon, J. J.; Tang, R.; Buhro, W. E.; Loomis, R. A. Synchronous Photoluminescence Intermittency (Blinking) along Whole Semiconductor Quantum Wires. *Nano Lett.* **2007**, *7*, 3290–3295.
15. Frantsuzov, P.; Kuno, M.; Jankó, B.; Marcus, R. A. Universal Emission Intermittency in Quantum Dots, Nanorods and Nanowires. *Nat. Phys.* **2008**, *4*, 519–522.
16. Wustholz, K. L.; Sluss, D. R. B.; Kahr, B.; Reid, P. J. Applications of Single-Molecule Microscopy to Problems in Dyed Composite Materials. *Int. Rev. Phys. Chem.* **2008**, *27*, 167–200.
17. Vogelsang, J.; Kasper, R.; Steinhauer, C.; Person, B.; Heilemann, M.; Sauer, M.; Tinnefeld, P. A Reducing and Oxidizing System Minimizes Photobleaching and Blinking of Fluorescent Dyes. *Angew. Chem., Int. Ed.* **2008**, *47*, 5465–5469.
18. Rezzonico, D.; Jazbinsek, M.; Bosshard, C.; Gunter, P.; Bale, D. H.; Liao, Y.; Dalton, L. R.; Reid, P. J. Photostability Studies of π-Conjugated Chromophores with Resonant and Nonresonant Light Excitation for Long-Life Polymeric Telecommunication Devices. *J. Opt. Am. Soc. B* **2007**, *24*, 2199–2207.
19. Veerman, J. A.; Garcia-Parajo, M. F.; Kuipers, L.; van Hulst, N. F. Time-Varying Triplet State Lifetimes of Single Molecules. *Phy. Rev. Lett.* **1999**, *83*, 2155–2158.
20. Kulzer, F.; Kummer, S.; Basche, T.; Brauchle, C. Quantum Jumps of Single Molecules: A Method to Measure Triplet Kinetics. *J. Inform. Rec.* **1996**, *22*, 567–572.
21. Bernard, J.; Fleury, L.; Talon, H.; Orrit, M. Photon Bunching in the Fluorescence from Single Molecules—A Probe for Intersystem Crossing. *J. Chem. Phys.* **1993**, *98*, 850–859.
22. Köhn, F.; Hofkens, J.; Gronheid, R.; Van der Auweraer, M.; De Schryver, F. C. Parameters Influencing the On- and Off-Times in the Fluorescence Intensity Traces of Single Cyanine Dye Molecules. *J. Phys. Chem. A* **2002**, *106*, 4808–4814.
23. Wustholz, K. L.; Bott, E. D.; Isborn, C. M.; Li, X.; Kahr, B.; Reid, P. J. Dispersive Kinetics from Single Molecules Oriented in Single Crystals of Potassium Acid Phthalate. *J. Phys. Chem. C* **2007**, *111*, 9146–9156.
24. Haase, M.; Hubner, C. G.; Reuther, E.; Herrmann, A.; Mullen, K.; Basche, T. Exponential and Power-Law Kinetics in Single-Molecule Fluorescence Intermittency. *J. Phys. Chem. B* **2004**, *108*, 10445–10450.
25. Osad'ko, I. S. Room-Temperature Fluctuations in the Fluorescence of a Single Polymer Molecule. *J. Exp. Theor. Phys.* **2003**, *96*, 617–628.
26. Weston, K. D.; Buratto, S. K. Millisecond Intensity Fluctuations of Single Molecules at Room Temperature. *J. Phys. Chem. A* **1998**, *102*, 3635–3638.
27. Yeow, E. K. L.; Melnikov, S. M.; Bell, T. D. M.; De Schryver, F. C.; Hofkens, J. Characterizing the Fluorescence Intermittency and Photobleaching Kinetics of Dye Molecules Immobilized on a Glass Surface. *J. Phys. Chem. A* **2006**, *110*, 1726–1734.
28. Kuno, M.; Fromm, D. P.; Johnson, S. T.; Gallagher, A.; Nesbitt, D. J. Modeling Distributed Kinetics in Isolated Semiconductor Quantum Dots. *Phys. Rev. B* **2003**, 67.
29. Heilemann, M.; Dedecker, P.; Hofkens, J.; Sauer, M. Photoswitches: Key Molecules for Subdiffraction-Resolution Fluorescence Imaging and Molecular Quantification. *Laser Photon. Rev.* **2009**, *3*, 180–202.
30. Andresen, M.; Stiel, A. C.; Trowitzsch, S.; Weber, G.; Eggeling, C.; Wahl, M. C.; Hell, S. W.; Jakobs, S. Structural Basis for Reversible Photoswitching in Dronpa. *Proc. Natl. Acad. Sci. U.S.A.* **2007**, *104*, 13005–13009.
31. Clifford, J. N.; Bell, T. D. M.; Tinnefeld, P.; Heilemann, M.; Melnikov, S. M.; Hotta, J.; Sliwa, M.; Dedecker, P.; Sauer, M.; Hofkens, J.; Yeow, E. K. L. Fluorescence of Single Molecules in Polymer Films: Sensitivity of Blinking to Local Environment. *J. Phys. Chem. B* **2007**, *111*, 6987–6991.
32. Vogelsang, J.; Cordes, T.; Forthmann, C.; Steinhauer, C.; Tinnefeld, P. Controlling the Fluorescence of Ordinary Oxazine Dyes for Single-Molecule Switching and Superresolution Microscopy. *Proc. Natl. Acad. Sci. U.S.A.* **2009**, *106*, 8107–8112.
33. Vogelsang, J.; Cordes, T.; Tinnefeld, P. Single-Molecule Photophysics of Oxazines on DNA and Its Application in a FRET Switch. *Photochem. Photobiol. Sci.* **2009**, *8*, 486–496.
34. Wang, X.; Ren, X.; Kahen, K.; Hahn, M. A.; Rajeswaran, M.; Maccagnano-Zacher, S.; Silcox, J.; Cragg, G. E.; Efros, A. L.; Krauss, T. D. Non-Blinking Semiconductor Nanocrystals. *Nature* **2009**, *459*, 686−689.
35. Benedict, J. R.; Wallace, P. M.; Reid, P. J.; Jang, S. H.; Kahr, B. Up-Conversion Luminescence in Dye-Doped Crystals of Potassium Hydrogen Phthalate. *Adv. Mater.* **2003**, *15*, 1068.
36. Barbon, A.; Bellinazzi, M.; Benedict, J. B.; Brustolon, M.; Fleming, S. D.; Jang, S. H.; Kahr, B.; Rohl, A. L. Luminescent Probes of Crystal Growth: Surface Charge and Polar Axis Sense in Dye-Doped Potassium Hydrogen Phthalate. *Angew. Chem., Int. Ed.* **2004**, *43*, 5328–5331.

37. Bullard, T.; Wustholz, K. L.; Bott, E. D.; Robertson, M.; Reid, P. J.; Kahr, B. Role of Kinks in Dyeing Crystals: Confocal Luminescence Microscopy from Single Molecules to Square Centimeters. *Cryst. Growth Des.* **2009**, *9*, 982–990.
38. Wustholz, K. L.; Bott, E. D.; Kahr, B.; Reid, P. J. Memory and Spectral Diffusion in Single-Molecule Emission. *J. Phys. Chem. C* **2008**, *112*, 7877−7885.
39. Kahr, B.; Gurney, R. W. Dyeing Crystals. *Chem. Rev.* **2001**, *101*, 893–951.
40. Guttler, F.; Croci, M.; Renn, A.; Wild, U. P. Single Molecule Polarization Spectroscopy: Pentacene in *p*-Terphenyl. *Chem. Phys.* **1996**, *211*, 421–430.
41. Walla, P. J.; Jelezko, F.; Tamarat, P.; Lounis, B.; Orrit, M. Perylene in Biphenyl and Anthracene Crystals: An Example of the Influence of the Host on Single-Molecule Signals. *Chem. Phys.* **1998**, *233*, 117–125.
42. Neuhauser, R. G.; Shimizu, K. T.; Woo, W. K.; Empedocles, S. A.; Bawendi, M. G. Correlation between Fluorescence Intermittency and Spectral Diffusion in Single Semiconductor Quantum Dots. *Phys. Rev. Lett.* **2000**, *85*, 3301–3304.
43. Stracke, F.; Blum, C.; Becker, S.; Mullen, K.; Meixner, A. J. Correlation of Emission Intensity and Spectral Diffusion in Room Temperature Single-Molecule Spectroscopy. *ChemPhysChem* **2005**, *6*, 1242–1246.
44. Tang, J.; Marcus, R. A. Mechanisms of Fluorescence Blinking in Semiconductor Nanocrystal Quantum Dots. *J. Chem. Phys.* **2005**, 123.
45. Verberk, R.; van Oijen, A. M.; Orrit, M. Simple Model for the Power-Law Blinking of Single Semiconductor Nanocrystals. *Phys. Rev. B* **2002**, *66*.
46. Sher, P. H.; Smith, J. M.; Dalgarno, P. A.; Warburton, R. J.; Chen, X.; Dobson, P. J.; Daniels, S. M.; Pickett, N. L.; O'Brien, P. Power Law Carrier Dynamics in Semiconductor Nanocrystals at Nanosecond Timescales. *Appl. Phys. Lett.* **2008**, 92.
47. Schlegel, G.; Bohnenberger, J.; Potapova, I.; Mews, A. Fluorescence Decay Time of Single Semiconductor Nanocrystals. *Phys. Rev. Lett.* **2002**, 88.
48. Fisher, B. R.; Eisler, H. J.; Stott, N. E.; Bawendi, M. G. Emission Intensity Dependence and Single-Exponential Behavior in Single Colloidal Quantum Dot Fluorescence Lifetimes. *J. Phys. Chem. B* **2004**, *108*, 143–148.
49. Berberan-Santos, M. N.; Bodunov, E. N.; Valeur, B. Mathematical Functions for the Analysis of Luminescence Decays with Underlying Distributions 1. Kohlrausch Decay Function (Stretched Exponential). *Chem. Phys.* **2005**, *315*, 171–182.
50. Fomenko, V.; Nesbitt, D. J. Solution Control of Radiative and Nonradiative Lifetimes: A Novel Contribution to Quantum Dot Blinking Suppression. *Nano Lett.* **2008**, *8*, 287–293.
51. Fu, Y.; Zhang, J.; Lakowicz, J. R. Suppressed Blinking in Single Quantum Dots (QDs) Immobilized near Silver Island Films (SIFs). *Chem. Phys. Lett.* **2007**, *447*, 96–100.
52. Montiel, D.; Yang, H. Observation of Correlated Emission Intensity and Polarization Fluctuations in Single CdSe/ZnS Quantum Dots. *J. Phys. Chem. A* **2008**, *112*, 9352–9355.
53. Barkai, E.; Jung, Y. J.; Silbey, R. Theory of Single-Molecule Spectroscopy: Beyond the Ensemble Average. *Annu. Rev. Phys. Chem.* **2004**, *55*, 457–507.
54. Sluss, D. R. B.; Bingham, C.; Burr, M.; Bott, E. D.; Riley, E. A.; Reid, P. J. Temperature Dependent Fluorescence Intermittency for Single Molecules of Violamine R in Poly(vinyl alcohol). *Chem. Mater.* In press.
55. Watkins, L. P.; Yang, H. Detection of Intensity Change Points in Time-Resolved Single-Molecule Measurements. *J. Phys. Chem. B* **2005**, *109*, 617–628.
56. McHedlov-Petrossyan, N. O.; Rubtsov, M. I.; Lukatskaya, L. L. Ionization and Tautomerism of Chloro-Derivatives of Fluorescein in Water and Aqueous Acetone. *Dyes Pigment* **1992**, *18*, 179–198.
57. Horst Leonhardt, L. G.; Livingston, R. Acid−Base Equilibria of Fluorescein and 2′,7′-Dichlorofluorescein in Their Ground and Fluorescent States. *J. Phys. Chem.* **1971**, *75*, 245–249.
58. Zondervan, R.; Kulzer, F.; Orlinskii, S. B.; Orrit, M. Photoblinking of Rhodamine 6G in Poly(vinyl alcohol): Radical Dark State Formed through the Triplet. *J. Phys. Chem. A* **2003**, *107*, 6770–6776.
59. Lougnot, D. J.; Goldschmidt, C. R. Photoionization of Fluorescein *via* Excited Triplet and Singlet States. *J. Photochem.* **1980**, *12*, 215–224.
60. Leaver, I. H. ESR Study of Radical Intermediates in Photoreduction of Xanthene Dyes. *Aust. J. Chem.* **1971**, *24*, 753–763.
61. Marchesi, E.; Rota, C.; Fann, Y. C.; Chignell, C. F.; Mason, R. P. Photoreduction of the Fluorescent Dye 2′,7′-Dichlorofluorescein: A Spin Trapping and Direct Electron Spin Resonance Study with Implications for Oxidative Stress Measurements. *Free Radical Biol. Med.* **1999**, *26*, 148–161.
62. Orte, A.; Bermejo, R.; Talavera, E. M.; Crovetto, L.; Alvarez-Pez, J. M. 2′,7′-Difluorofluorescein Excited-State Proton Reactions: Correlation between Time-Resolved Emission and Steady-State Fluorescence Intensity. *J. Phys. Chem. A* **2005**, *109*, 2840–2846.
63. Orte, A.; Crovetto, L.; Talavera, E. M.; Boens, N.; Alvarez-Pez, J. M. Absorption and Emission Study of 2′,7′-Difluorofluorescein and Its Excited-State Buffer-Mediated Proton Exchange Reactions. *J. Phys. Chem. A* **2005**, *109*, 734–747.
64. Orte, A.; Talavera, E. M.; Macanita, A. L.; Orte, J. C.; Alvarez-Pez, J. M. Three-State 2′,7′-Difluorofluorescein Excited-State Proton Transfer Reactions in Moderately Acidic and Very Acidic Media. *J. Phys. Chem. A* **2005**, *109*, 8705–8718.
65. Varma, K. B. R.; Raju, A. R.; Rao, J. Physico-Chemical Properties of Pure and X-ray Irradiated Single Crystals of KAP. *Cryst. Res. Technol.* **1988**, *23*, 185–193.
66. Wustholz, K. L.; Kahr, B.; Reid, P. J. Single-Molecule Orientations in Dyed Salt Crystals. *J. Phys. Chem. B* **2005**, *109*, 16357–16362.
67. McHedlov-Petrossyan, N. O.; Salamanova, N. V.; Vodolazkaya, N. A.; Gurina, Y. A.; Borodenko, V. I. A Dibasic Acid with Reversed Order of the Stepwise Ionization Constants: 2,7-Dichlorofluorescein in the Ternary Solvent Mixture Benzene-Ethanol-Water. *J. Phys. Org. Chem.* **2006**, *19*, 365–375.